The excitonic Zeeman effect in uniaxially-strained germanium

G. N. Gol'tsman, É. N. Gusinskiĭ, A. V. Malyavkin, N. G. Ptitsina, A. G. Selevko, and
V. M. Édel'shtein

V. I. Lenin State Teachers' Institute, Moscow

We have carried out a high-resolution spectroscopic study of the absorption of submillimeter radiation by free excitons in germanium compressed along the [111] axis in a magnetic field parallel to the compression axis. In particular, we studied the splitting of the $1s \to 2p$ transition in fields up to 6 kOe at $T = 1.6$ K, and observed a complex pattern in the Zeeman splitting which we believe is related to the effect of thermal motion of the excitons in a magnetic field on their internal structure (the magneto-Stark effect). The calculated submillimeter spectrum of excitons agrees with the experimental data. We predict that in a magnetic field the energy of the $2p_{-1}$ term is a minimum at a finite value of the exciton momentum perpendicular to the field—that is, the energy minimum forms a ring in momentum space. It follows that the density of states for this term must be a nonmonotonic function of the energy. A theory is developed of analogous phenomena in positronium.

INTRODUCTION

Experiments in the submillimeter-wave region provide the most complete information on the energy structure of excitons, since energies in this region correspond to the excitonic binding energy. However, the results of experiments of this kind carried out in unstrained germanium[1-5] are generally in rather poor agreement with the corresponding theoretical calculations.[6] The difficulty in interpreting the spectra theoretically reflects the complexity of the band structure of unstrained germanium.

Application of uniaxial strain significantly simplifies the band structure of Ge. In the limit of strong compression along the [111] direction, the excitonic states are built out of one electron valley and one hole valley; both valleys are ellipsoids of rotation with principal axes along [111]. In this case the exciton structure becomes hydrogenic, and consequently is easier to interpret. This fact is confirmed in particular by the results given in Ref. 7, where the $1s \to 2p$ and $1s \to 3p$ exciton transitions were studied in germanium strongly compressed along the [111] axis (the pressure satisfies $F \leqslant 400$ MPa). The observed energy ε and intensity of these transitions agree with the hydrogenic model.

If we apply a weak magnetic field to Ge under these conditions (we will consider the most symmetric case, where the directions of the field and strain coincide), then from what was discussed above we should expect the $1s \to 2p$ transitions to be split according to the normal Zeeman effect, i.e., one π-component should appear which undergoes only a quadratic shift with field, and two σ-components which shift linearly with field. In contrast, the splitting we observe presents a much more complex picture.

We know of one experimental paper[8] devoted to the Zeeman effect in uniaxially-strained Ge. Because its authors, in studying the exciton spectrum of Ge, restricted themselves to rather strong fields, they came to the conclusion that this spectrum could be described by a very simple theory. However, as we will show, they did not observe all the components of the $1s \to 2p$ multiplet, and incorrectly interpreted one of the three transitions they observed.

An analysis of the spectral data obtained in this paper shows that the basic source of complexity in these spectra is the thermal motion of the excitons. We also found that even at helium temperatures the spin-orbit energy of the holes has some influence on the spectrum, despite the strong compression.

When moving in a magnetic field, the exciton, which in contrast to a charged electron is a neutral entity, possesses a momentum which to first order is conserved; however, the energy spectrum of internal motion of the particles does in fact depend on the exciton velocity. This is easy to understand if we go to a frame of reference in which the exciton is at rest: in a magnetic field **H**, an electric field **E** appears in the exciton rest frame which is perpendicular to the exciton's velocity of thermal motion **v** in the laboratory system:

$$\mathbf{E} = [\mathbf{v}/c, \mathbf{H}], \tag{1}$$

This electric field gives rise to a Stark effect (the "magneto-Stark effect"), a fact which was first noted in Ref. 9 and applied to the hydrogen atom. The Stark field affects the optical properties of ground-state excitons in a number of ways, some of which were studied in Refs. 10–13. Since the magnitude of the field E is determined by the velocity v and consequently by the atomic mass, while the internal energetic structure is determined by the mass of a light particle, i.e., the electron, the effect of this field is very small in the hydrogen atom. A much stronger magneto-Stark effect should occur in the energy spectrum of lighter atoms, e.g., positronium; the effect should be even stronger in Wannier-Mott excitons in semiconductors, because of the still smaller effective masses of electrons and holes, which are in addition comparable in magnitude, and because of the large dielectric constant of the crystal $\varkappa$.

The electric field mixes wave functions with opposite spatial parities; hence, it mixes some of the excited p-states into the $1s$ ground state. From this it is clear that for exciton states with principal quantum number $n = 2$ the effect is enhanced still more by the fact that now the close-lying $2s$

and $2p_{\pm 1}$ states can mix; as we will show below, strong mixing of this kind can occur even at low frequencies and in relatively weak magnetic fields.

Any experiment which probes the energy spectrum of an exciton will also give information about the spectrum of positronium. It is well known that for $T = 0$, the spectra of positronium and excitons made up of equal-mass electrons and holes must coincide when expressed in reduced units of energy ε/R_y (R_y is the effective Rydberg) and magnetic field $\hbar\omega_c$ (ω_c is the cyclotron frequency). It is found that this agreement is also observed in the case of thermal motion, although the spectra themselves are considerably more complicated. In addition, as we will show below, the magneto-Stark effect leads to nontrivial features in the behavior of a number of states (e.g., $2p_{-1}$) both in the exciton and in positronium.

After a detailed study of the excitonic Zeeman effect in Ge under uniaxial compression, we became convinced that the magneto-Stark effect, although the fundamental cause, was not the only cause of the complexity of the spectrum. There is another considerably weaker effect which is characteristic of excitons in Ge under strong compression but not of positronium.

It is well known that the fourfold-degenerate valence band of Ge corresponding to an angular momentum $J = 3/2$ is split into two bands with angular momentum projections $M = \pm 1/2$ and $M = \pm 3/2$ when a uniaxial compression is applied along the [111] axis. For the maximum attainable pressure $F \approx 400$ MPa, at which the crystal strain still retains a high degree of homogeneity, the magnitude of this splitting reaches a value of 14.6 meV. This is much smaller than the transition energies to the other bands; hence, the external magnetic field can cause virtual hole transitions between these two bands, leading to various corrections to the quadratic dispersion law for holes. With regard to the Zeeman effect, the most interesting of these corrections (and therefore the ones we studied) are those which cause the hole g-factors to depend on the quantum numbers of the internal states of the exciton, i.e., on their kinetic energy within the exciton.

2. SPECTRUM OF EXCITON EXCITED STATES IN A MAGNETIC FIELD

Let us start by making some necessary estimates of matrix elements for those physical quantities which characterize the excited states of excitons in a magnetic field. We choose a coordinate system with the z-axis along the [111] direction. In crystals of Ge strained along this axis, the Hamiltonian which describes an exciton moving with momentum $\mathbf{k}$, including only one hole band with $M_J = \pm 1/2$, has the form

$$\mathcal{H} = \varepsilon_k + \mathcal{H}_0 + \mathcal{H}_m + \mathcal{H}_{sp} + \mathcal{H}_{\mu s},$$

$$\varepsilon_k = \frac{k_\perp^2}{2M_\perp} + \frac{k_z^2}{2M_\parallel},$$

$$\mathcal{H}_0 = \frac{\mathbf{p}^2}{2\mu} - \frac{e^2}{\varkappa r} - \frac{\beta}{3\mu}(\mathbf{p}^2 - 3p_z^2),$$

$$\mathcal{H}_m = \frac{e\hbar}{2\mu_\perp c}\gamma\mathbf{H}[\mathbf{rp}] + \frac{e^2}{8\mu_\perp c^2}H^2 r^2 \sin^2\theta,$$

$$\mathcal{H}_{sp} = \mu_B H(\sigma_{ez} + \sigma_{hz}),$$

$$\mathcal{H}_{\mu s} = \frac{e\hbar}{\mu_\perp c}[\mathbf{kH}]\mathbf{r},$$

(2)

where

$$\frac{1}{\mu} = \frac{2}{3\mu_\perp} + \frac{1}{3\mu_\parallel}, \quad \beta = \frac{\mu}{2}\left(\frac{1}{\mu_\parallel} - \frac{1}{\mu_\perp}\right),$$

$$\mu_B = \frac{e\hbar}{2m_0 c}, \quad \gamma = \frac{m_h - m_e}{m_h + m_e}.$$

Here, ε_k is the kinetic energy of translational motion, and $\mu_\parallel$ and $\mu_\perp$ are components of the reduced effective mass tensor of the exciton. The operator $\mathcal{H}_0$ determines the spectrum of internal motion in the absence of a magnetic field; for germanium under a compression of $F = 400$ MPa, $m_0/\mu_\parallel = 25.6$, $m_0/\mu_\perp = 19.9$, $m_0/\mu = 21.8$, $\gamma = 0.24$, $\beta = 0.131$ and the next term in $\mathcal{H}_0$ is a small correction. The operator $\mathcal{H}_m$ describes the effect of the magnetic field on the orbital motion within the exciton. Here we choose to analyze only those parts of the spectra where the magnetic field can be considered weak; if by "weak" we mean that the corrections to the energy from $\mathcal{H}_m$ must not exceed $\varepsilon_{3s} - \varepsilon_{2s}$, then we find $H \lesssim 2$ kOe. The main difference between the Hamiltonian $\mathcal{H}_m$ and the analogous atomic Hamiltonian is the presence of a small numerical factor $\gamma = 0.24$ in the term linear in the field. For the $2s$ and $2p$ exciton excited states, in which the mean square size of the exciton bound-state region is several times larger than in the ground state, the term quadratic in field is comparable to the linear term even at fields ≈ 1 kOe. The Hamiltonian $\mathcal{H}_{sp}$ determines the interaction energy between the electron and hole spins in a magnetic field, while $\mathcal{H}_{\mu s}$ corresponds to the magneto-Stark effect mentioned in the Introduction.

If we take into consideration the finite value of the hole band splitting Δ_h and the possibility of virtual interband transitions under the influence of the magnetic field, then we obtain the following correction to the Hamiltonian (2):

$$\delta\mathcal{H} = \delta\mathcal{H}_g + \delta\mathcal{H}_{so},$$
$$\delta\mathcal{H}_g = 2(\mu_B H/\Delta_h)m_0\sigma_z[(2\gamma_2^2 + \gamma_3^2)p_z^2 - (\gamma_2^2 + 2\gamma_3^2)\mathbf{p}_\perp^2],$$
$$\delta\mathcal{H}_{so} = 12(\mu_B H/\Delta_h)m_0\gamma_2\gamma_3 p_z(p_+\sigma_+ - p_-\sigma_-),$$

(3)

where $\gamma_{2,3}$ are the Luttinger band parameters[14], $m_0\gamma_2 = 4.25$, $m_0\gamma_3 = 5.69$ [14], $p_\pm = p_x \pm ip_y$, $\sigma_\pm = 1/2(\sigma_x \pm i\sigma_y)$. The Hamiltonian $\delta\mathcal{H}_g$ leads to a dependence of the hole g-factor on the quantum numbers of the exciton's internal motion, while $\delta\mathcal{H}_{so}$ mixes certain levels with different spin and orbital angular momentum. Generally speaking, we should also include terms quadratic in the field in the Hamiltonian $\delta\mathcal{H}$; however, in contrast to the Hamiltonian $\mathcal{H}_m$, here these terms are small compared to the linear terms, since the latter do not have the small factor γ. The effect of the Hamiltonian $\delta\mathcal{H}$ on the spectrum is smaller than that of $\mathcal{H}_m$, essentially by a factor of R_y/Δ_h. Under our experimental conditions we have $R_y = (\mu e^4/2\varkappa^2\hbar^2) = 2.63$ MeV, $\varkappa = 15.36$ [15], $\Delta_h = 14.6$ MeV,[15] so that $R_y/\Delta_h = 0.18$.

Let us estimate the values of various energies and matrix elements for the p-states with principal quantum number $n = 2$. Because of the anisotropy of the reduced effective mass (the third term in the Hamiltonian $\mathcal{H}_0$), the excited levels are split. Their energies, measured from the unperturbed energy $R_y/4$, equal

$$\delta\varepsilon = (1 - 3m^2/2)\, 2\beta R_y/15, \tag{4}$$

where the magnetic quantum number is $m = 0,\ \pm 1$. The energy of the 2s-level remains equal to $R_y/4$. The energy difference $\varepsilon_{2p_0} - \varepsilon_{2p_{\pm 1}} = 69\ \mu\text{eV}$ serves as a characteristic energy scale for the Zeeman effect studied here at fields $H \lesssim 2$ kOe.

The matrix elements of $\delta\mathscr{H}_{s0}$ are nonvanishing only between the states $2p_0$ and $2p_{\pm 1}$. The value of this matrix element, found by using hydrogenic wave functions (HWFs) is

$$\langle 2p_0 | \delta\mathscr{H}_{s0} | 2p_{\pm 1} \rangle = \frac{2,4}{2^{\frac{1}{2}}} (m_0 \gamma_2 \gamma_3 \mu)\, \frac{R_y}{\Delta_h} (\mu_B H). \tag{5}$$

In a field $H = 1$ kOe, this is approximately $2\ \mu\text{eV}$, i.e., so small that $\delta\mathscr{H}_{s0}$ need be included only within the narrow region where unperturbed terms intersect.

From Eq. (3) we can obtain expressions for the mean values of the operator $\delta\mathscr{H}_g$ in various exciton states:

$$\langle 1s | \delta\mathscr{H}_g | 1s \rangle = -6\sigma_{zh}(\mu_B H)\, \frac{R_y}{\Delta_h},$$

$$\langle 2s | \delta\mathscr{H}_g | 2s \rangle = -1,67\sigma_{zh}(\mu_B H)\, \frac{R_y}{\Delta_h},$$

$$\langle 2p_0 | \delta\mathscr{H}_g | 2p_0 \rangle = 0,37\sigma_{zh}(\mu_B H)\, \frac{R_y}{\Delta_h}, \tag{6}$$

$$\langle 2p_{\pm 1} | \delta\mathscr{H}_g | 2p_{\pm 1} \rangle = -2,42\sigma_{zh}(\mu_B H)\, \frac{R_y}{\Delta_h}.$$

It is obvious that there is a very large difference in the g-factors of holes for the ground and $2p_0$ states; the splitting of the $1s - 2p_0$ transition amounts to $13.3\ \mu\text{eV}$ for $H = 1$ kOe.

The operator $\mathscr{H}_{\mu s}$ mixes the $2p_{\pm 1}$ and $2s$ states, but does not affect the $2p_0$ state. It is easy to verify that

$$\langle 2s | \mathscr{H}_{\mu s} | 2p_{\pm 1} \rangle = \frac{3aev_{\pm}}{2^{\frac{1}{2}}c} H, \tag{7}$$

where $v_{\perp} = k_{\perp}/M_{\perp}$ is the velocity of the center-of-mass motion of the exciton, $v_{\pm} = v_x \pm iv_y$, $a = \varkappa\hbar^2/me^2 = 177$ Å. At a temperature of 1.6 K and a mass $M_{\perp} = 0.21\, m_0$, the mean value of the squared component of thermal velocity equals $|v_x^2| = 1.45 \times 10^{12}\ (\text{cm/sec})^2$. From this it follows that

$$\langle 2s | \mathscr{H}_{\mu s} | 2p_{\pm 1} \rangle = 7\,(\mu_B H)\, \frac{v_x \pm iv_y}{|v_x^2|^{\frac{1}{2}}}. \tag{8}$$

In a magnetic field $H = 1$ kOe and $T = 1.6$ K, the magnitude of this matrix element for an exciton moving at the mean thermal velocity equals $42\ \mu\text{eV}$. This small value requires that the correct linear combinations of $2p_{\pm 1}$, $2s$ states for the moving exciton be found by solving the corresponding secular equation.

3. EXPERIMENTAL METHOD

We found that it was possible to observe the narrow exciton transition lines from the ground state to excited states, and to obtain the precise energy spectrum and its variation with magnetic field, if we first imposed some preliminary requirements on the apparatus and experimental conditions; primarily, the sample strain must be endowed with a

high degree of homogeneity and the excitation must allow establishment of quasi-equilibrium conditions, i.e., the levels of probe radiation, and of the light which creates free excitons, should be so low that the exciton distribution function is one of thermal equilibrium. Violation of these conditions causes broadening of the spectral lines (as experiment shows) and reduces the accuracy of the measurements. Study of the exciton spectra under these conditions calls for the use of a sensitive spectrometer with high resolution.

Our investigations of the exciton spectra in Ge were carried out in the submillimeter-wave region, using a spectrometer with a backward-wave oscillator (BWO) tube at a temperature of 1.6 K. The pressure and magnetic field were applied along the [111] axis of the crystal. Uniaxial strain was produced by the method described in Ref. 16. A sample with dimensions $2.5 \times 2.5 \times 10$ mm³, oriented along the [111] axis, was fitted between spacers made of lead-tin alloy, which provided a high degree of homogeneity of the strain up to a pressure of ≈ 400 MPa. Excitons were generated by volume excitation of the sample with light in the region of interband absorption, using an incandescent lamp with filters. The exciton concentration could be varied from 10^{10} to 10^{12} cm⁻³. The submillimeter radiation and light were supplied to the sample through an optical window in the cryostat across a gap in the superconducting Helmholtz coils used for the magnetic-field experiments. In order to simplify the form of the spectrum and identify the lines, the experiments were carried out using linearly-polarized light; the electric component $\mathbf{E}_-$ of the wave field was oriented parallel or perpendicular to the crystal [111] axis. The submillimeter radiation passing through the sample arrived at an n-InSb detector, which was taken outside the limits of the magnetic field and covered by a filter of black paper, so as to avoid the effect of the interband light on it. In order to measure the absorption spectra of light which was exciting the excitons, we modulated it with a chopper, and extracted from the detector a signal proportional to the absorption coefficient. The photoconductivity was recorded under continuous illumination by modulating the submillimeter radiation; we deposited ohmic contacts on the sample to do this. In order to record the spectra in the absence of a magnetic field as the frequency of the BWO tube radiation was scanned, we used automatic power stabilization.[17] In studying the Zeeman effect, the spectra were "unrolled" by varying the magnetic field for a fixed frequency of the BWO tube radiation. The method of recording the spectra is described in more detail in Ref. 2.

In these investigations we used samples which were as pure as possible, with a total concentration of residual impurities $\lesssim 10^{12}$ cm⁻³; the lifetime of excitons in these strained samples amounted to $\approx 10\ \mu\text{sec}$.

4. EXPERIMENTAL RESULTS

In Fig. 1 we show a portion of the absorption spectrum of strained Ge ($F = 400$ MPa) for two polarizations of the submillimeter radiation—$\mathbf{E}_-\perp F$(a) and $\mathbf{E}_-\|F$(b). We see two lines in the spectrum, whose relative intensities change sharply as the polarization of the radiation is switched. The position in the spectrum and characteristic polarization of the radiation indicates that the lines are associated with the $1s \to 2p_{\pm 1}$ and $1s \to 2p_0$ transitions. These data are in
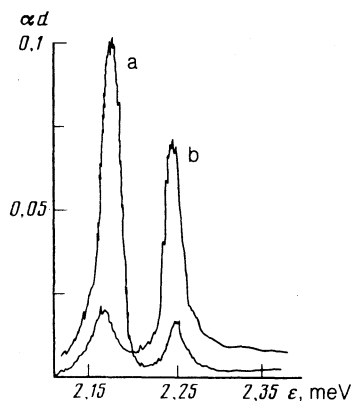
FIG. 1. Portion of the absorption spectrum of uniaxially-strained Ge for the polarizations $E_- \perp F$ (a) and $E_- \| F$ (b); $T = 1.6$ K, $H = 0$.
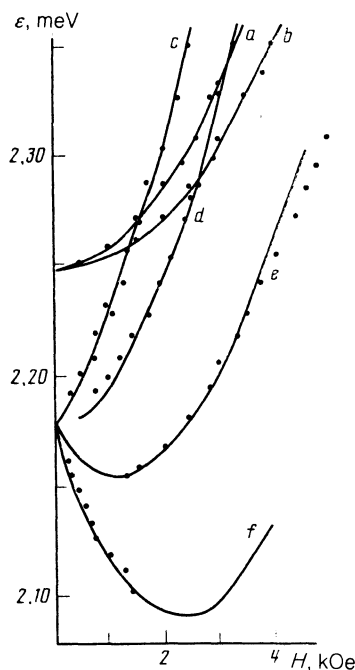

FIG. 2. Dependence of energy versus H for the transition seen in the absorption spectrum at $T = 1.6$ K. The continuous curves are calculations of the energies corresponding to the absorption maxima for left- and right-circular polarized radiation.

complete agreement with those presented in Ref. 7; however, the widths of the lines we observed were almost an order of magnitude smaller, amounting to ≈ 20 μeV. In observing the photoconductivity spectrum under the same conditions, we found a nonresonant band with a long-wavelength edge at $\varepsilon_0 \approx 2.8$ meV. The value of ε_0 depends strongly on the magnitude of the pressure: as F increases, ε_0 shifts to the low-energy side.

The lines in the absorption spectrum are split in a magnetic field (Fig. 2): the line corresponding to the $1s \to 2p_0$ transition, up to the largest magnetic field we used ($H \approx 10$ kOe) had two components denoted by a and b in Fig. 2 (the magnitude of the splitting for small H depends linearly on field, with a slope of $\approx 8 \pm 1$ μeV/kOe); the second line has a more complex structure. In weak fields (up to 0.5 kOe) we observe only two of its components (c and f); the d component appears clearly only in a field $H \gtrsim 0.8$ kOe. The intensity of the lower component f decreases rapidly as H increases, and at $H \gtrsim 1.5$ kOe this line is no longer visible in the spectrum; however, for $H \gtrsim 1$ kOe line (e) appears, whose intensity increases with H. It also is observed for the polarization $E_- \perp H$, F.

In Fig. 3, we show an example of three absorption spectra recorded at different energy quanta ε and radiation polarizations (a and b were for $E_- \perp H$, F, c for $E_- \| H$, F) by sweeping over H. The first includes the components f and e, the second c and d, and the third a and b. The large difference in widths for the lines a, b as compared to c, d, e is immediately apparent: the lines in the latter group are considerably wider, while the width of lines c and e is larger than that of d. In addition, components of the $1s \to 3p_{\pm 1}$ and $1s \to 3p_0$ lines show up clearly in a magnetic field, which allow us to deter-

mine the energies of these transitions for $H = 0$ with fair accuracy. The energies of all these transitions at $H = 0$ and $F = 400$ MPa are given in Table I.

5. DISCUSSION OF RESULTS

Let us first discuss the results for $H = 0$. Comparison with calculations shows that the energy difference of the observed transitions ($1s \to 2p_0$, $1s \to 2p_{\pm 1}$, $1s \to 3p_0$, $1s \to 3p_{\pm 1}$) are in very good agreement with theory (see Table I); however, the energies themselves differ from the theoretical values. This situation is typical, e.g., for shallow donors, and is connected with substantial central-cell corrections to the energies of the even-parity states, and especially to the ground-state energy; at the same time, the odd-parity states do not undergo a shift, and their energies agree with calculations within the effective-mass approximation. This mechanism should give rise to similar corrections to the energies of even-parity excitonic states. Therefore, it is only possible to determine the energy of the $1s$-state of an exciton accurately from the experimental data, just as for shallow donors; however,

TABLE I.

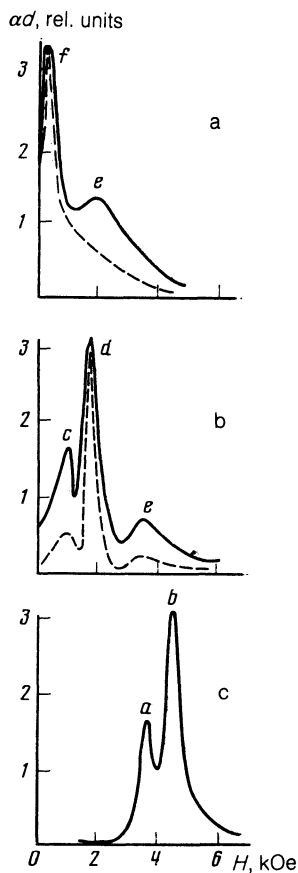| Notation for transitions	ε_{exp}, meV	ε_{theor}, meV
$1s \to 2p_0$	2.248	2.019
$1s \to 2p_{\pm 1}$	2.178	1.950
$1s \to 3p_0$	2.585	2.358
$1s \to 3p_{\pm 1}$	2.555	2.328
$(1s \to 2p_0) - (1s \to 2p_{\pm 1})$	0.070	0.069
$(1s \to 3p_0) - (1s \to 3p_{\pm 1})$	0.030	0.030
$(1s \to 3p_0) - (1s \to 2p_{\pm 1})$	0.407	0.408
$(1s \to 3p_{\pm 1}) - (1s \to 2p_{\pm 1})$	0.377	0.378

FIG. 3. Absorption spectra for uniaxially-strained Ge in a magnetic field at $T = 1.6$ K; a—$E_- \perp H$, F, $\varepsilon = 2.168$ meV; b—$E_- \perp H$, F, $\varepsilon = 2.228$ meV; c—$E_- \parallel H$, F, $\varepsilon = 2.373$ meV. The experimental spectra are shown as continuous curves, the calculations by dashed curves.

the energies of any of the p-states, e.g., $2p_{\pm 1}$, are well-predicted by the calculations and we can simply add on to them the corresponding transition energy. It is found that the binding energy of an exciton in Ge at $F = 400$ MPa comes to 2.86 meV, while its theoretical value according to effective-mass theory is 2.63 meV. The photoconductivity spectrum provides an independent way to determine the binding energy from the "red" side: $\varepsilon_0 = 2.8$ meV; both methods give similar results. These data also allow us to determine the energy of the $2s$ state. Let us note that the correction to the energy of the $2s$ state is 8 times smaller than that for the ground state, and thus the energy of the $2s$ state is found to be close to the energy of the $2p_{\pm 1}$ state. The energy levels calculated in this way are shown in Table II.

Let us turn now to a discussion of the effect of a magnetic field on the exciton absorption spectrum (Fig. 2). First of all, we note that the number of components in the $1s \rightarrow 2p$ multiplet is considerably larger than it should be for the normal Zeeman effect. In addition, the observed line width

differs considerably for different polarizations of the electromagnetic radiation ($E_- \perp H$ and $E_- \parallel H$).

As we noted above, the basic cause of this anomalous behavior of the Zeeman components is the magneto-Stark effect. The $2p_0$ state is practically unaffected; therefore, the transition line $1s \rightarrow 2p_0$ is significantly narrower than the others. Other than the quadratic shift $\Delta\varepsilon = (\alpha_{2p_0} - \alpha_{1s})H$,[2] this transition undergoes only the effect of the finite splitting of the valence band, which leads to a slight difference in the g-factors of the $1s$ and $2p_0$ states. The value of the linear-splitting constant calculated using (6) for this transition comes to 13.3 μeV/kOe; experiment gives a value of 8 ± 1 μeV/kOe, which is fairly close to this result. The remaining components of the $1s-2p$ multiplet must undergo still smaller splittings of this type, but since the lines corresponding to them are wider, they cannot be measured in practice.

It should be pointed out that the quadratic shift in the transition $1s \rightarrow 2p_0$ cannot be calculated accurately using HWFs: the average value of $\alpha_{2p_0} - \alpha_{1s}$ for the two components turns out to be smaller than the calculated value by a factor of 1.4. Possibly this is related to the fact that the real wave function for an excitonic excited state with anisotropic reduced mass differs from a HWF; this should give rise to a change in the diamagnetic shift constant. In Ref. 18, where a calculation is carried out of the diamagnetic susceptibility of exciton $1s$ states in strained Ge using the variational wave function of Ref. 19, it is shown that α_{1s} is 1.15 times smaller than for the case of using HWFs. We can be confident that a correct account of the anisotropic effective mass of the exciton will lead to a smaller theoretical value of the diamagnetic shift constant for the other states, too. However, there could be other reasons why α decreases. We emphasize that in all the calculations which follow we have chosen a value for α_{1s} in agreement with Ref. 18, while for $\alpha_{2p_{\pm 1}}$ and α_{2s} we picked values half as large as the values obtained by using HWFs. As will become clear, this value of the fitting parameter (chosen to be the same for both states, since α_{1s} and $\alpha_{2p_{\pm 1}}$ are close for HWFs) allows us to obtain very good agreement between theory and experiment for all the observed features of the Zeeman components when the radiation polarization is $E_- \perp H$.

As we noted earlier, the aggregate of all these results can be explained almost completely by the influence of the magneto-Stark effect. In fact, estimates show that due to the strong mixing of the $2p_{\pm 1}$ and $2s$ states the intensities of all three transitions can become comparable even in a fairly week field; hence, we now can understand the behavior of the new line (d) for $H \gtrsim 0.8$ kOe. The energy of the levels should be most strongly perturbed in the region where the terms are close to each other; far from this region, the position of one of the excited levels of the multiplet under discussion is found to be close to the $2s$ level for a stationary exciton, especially since it is located between the $2p_{+1}$ and $2p_{-1}$ levels, which

TABLE II.

Notation for levels	ε_{exp}, meV	ε_{theor}, meV	Notation for levels	ε_{exp}, meV	ε_{theor}, meV
$1s$	2.860	2.630	$2p_0$	0.610	0.611
$2s$	0.686	0.656	$3p_{\pm 1}$	0.303	0.302
$2p_{\pm 1}$	0.680	0.680	$3p_0$	0.273	0.272

shift it to different positions because of the magneto-Stark effect. When the energy of the lines is plotted as a function of H^2, it becomes apparent that the one which appears in the spectra for $H \gtrsim 0.8$ kOe follows a straight line in the region 1 kOe $< H < 2.5$ kOe. Prolonging this straight line to its intercept with the ordinate gives an energy of $2.178 \pm 2\mu$eV, very close to the value obtained above for the difference in energies of the $1s$ and $2s$ levels at $H = 0$ (2.175 meV). The fact that one of these lines practically coincides with the transition $1s \to 2s$, which is forbidden to the stationary exciton in this field region, is also implied by the results of calculations of the excitonic energy in the mixed $2p_{\pm 1}$, $2s$ states as a function of the transverse momentum $\mathbf{k}_\perp$ components of excitonic-thermal motion in a magnetic field obtained by solving the corresponding secular equation (see Fig. 4; here $\mathbf{k}_\perp$ is given in units of $(2kTM_\perp)^{1/2}$, $H = 2$ kOe, $T = 1.6$ K). It is clear that the dispersion law for term 2, which corresponds to the $2s$ state of a stationary exciton, is actually close to the quadratic $k_\perp^2/2M_\perp$, whereas the dispersion law for the terms 1, 3 (transitions to the $2p_{\pm 1}$ levels) at $H = 0$ is strongly nonquadratic due to mixing of the states.

The shape of the absorption lines is calculated by averaging the spectra over a Maxwellian distribution of excitons (see the Appendix); the magnitude of the homogeneous broadening is chosen in accordance with the experimental data for the transition width of $1s - 2p_0$. The spectrum obtained from such a calculation differs substantially from that of an exciton at rest, since each of the three states is now a mixture of the hydrogenic states $2p_{+1}$, $2s$ and $2p_{-1}$, and the polarization selection rule no longer applies. In addition, because of the differing dependences of the excitation and ground state energies on the velocity of the exciton motion as a whole (Fig. 4), the lines broaden and have different positions in the spectrum for different polarizations of the radiation. All this can be seen, e.g., in Fig. 5, where we show spectra calculated numerically for left- and right-hand circularly-polarized radiation. The position of the most intense central component appears the same for both polarizations of the radiation and corresponds to the transition $1s \to 2s$, which is a forbidden energy for excitons at rest; the intensities and positions of the side components are strong functions of polarization. We note that the weak line corresonding to right-hand polarization (to the left of the central peak) appears more clearly than the analogous peak for left-hand polarization (to the right of the central peak); the intensities of these two lines decrease strongly as H increases.
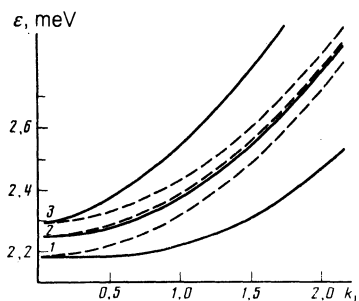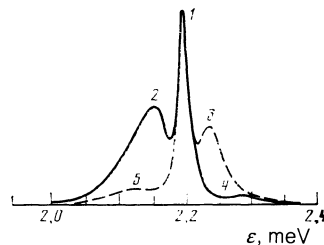
FIG. 5. Calculated absorption spectra for transitions to one of the mixed $2s$, $2p_{+1}$, $2p_{-1}$ states for left- (continuous curve) and right- (dashed curve) circular polarized radiation. $H = 1$ kOe, $T = 1.6$ K.

The difference in line widths in this spectrum is noteworthy: the central component has a width which does not differ much from that of the $1s - 2p_0$ transition at $H = 0$, while the remaining components undergo considerable inhomogeneous broadening which arise from the magneto-Stark effect and the Maxwellian velocity distribution of the excitons.

All these features in the calculated spectra can also be observed in experiment; however, they appear in an altered form: first, because in experiments which involve uniaxial compression the Zeeman effect cannot be induced when the Faraday configuration is used with circular polarization, so that it is necessary to use the Voigt configuration with linear polarization; second, because sweeping through the spectrum, i.e., varying the magnetic field at a given frequency of radiation, is more convenient to carry out. The first circumstance makes it impossible to observe all the weak lines described above over a wide range of H, while the second leads to strong variation in the relative line intensities in the spectra compared to "unrolling" in energy; this is due to the rather sharp dependence of certain of the line intensities on magnetic field. Therefore, in Fig. 3 we also present the results of calculations of the absorption spectrum as a function of magnetic field H for fixed energies corresponding to the experimental ones. It is now clear that the line shapes and intensity ratios for the experimental and theoretical spectra are close. We note that because of the sharp dependence of the intensities of lines e and f on H, line e is absent from the experimental spectrum in weak fields ($H \ll 1$ kOe), and the line f is absent in strong ones ($H > 1.5$ kOe).

In Fig. 2 we present a more detailed quantitative comparison of the results of calculations and experiments. Here, the calculated dependences of energy on field for the Zeeman components of the multiplet $1s \to 2p$ observed in experiment are shown as continuous lines. It is clear that in the weak-field region, the measured values of the energies of the observed lines practically coincide with the theoretical ones up to $H \lesssim 4$ kOe.

Experimental studies of the excitonic Zeeman effect in uniaxially strained Ge subjected to a magnetic field were also carried out, as we already mentioned, in Ref. 8. The actual resolution of the spectral lines reported there was considerably lower than that which we report here (possibly because of inhomogeneous compression). For this reason, and also because in Ref. 8 the number of lines generated by the laser and used in the spectrometer was insufficient,[8] the Zeeman effect could be studied only in fairly strong magnetic fields (5 to 70 kOe). In addition, it was not possible for these authors to observe all the components of the $1s - 2p$ multiplet: in their results, the lines e and f were absent, as was the splitting

FIG. 4. Calculated dependences of energy on $\mathbf{k}_\perp$ for exciton states corresponding to the $k = 0$ levels; 1—$2p_{-1}$, 2—$2s$, 3—$2p_{+1}$ (continuous curves). The same dependence without including the magneto-Stark effect is shown by dashed curves; $T = 1.6$ K, $H = 2$ kOe.

of the $1s - 2p_0$ transition. This led them to erroneous interpretations of the observed spectrum. The important influences of the magneto-Stark effect and the finite splitting of the valence band on the exciton spectrum in a magnetic field were not discussed, while only the absorption lines of the free excitons were ascribed to the magneto-Stark effect.

6. ANOMALOUS DISPERSION OF EXCITONS AND POSITRONIUM IN THE $2p_{-1}$ STATE

In addition to complicating the Zeeman spectrum as described above, the magneto-Stark effect also leads to features in the dispersion of certain excited states of excitons and positronium. Let us first consider the positronium atom. In the absence of a magnetic field, its kinetic energy varies quadratically with momentum for any quantum state of the internal motion. In a magnetic field, the position changes; so as to clarify the reason for anomalous dispersion of certain states, we will first neglect diamagnetic effects which are quadratic in the magnetic field. Then the energies of the $2s$ and $2p$ states of positronium coincide. Because of the magneto-Stark effect, a repulsion occurs between the $2p_{\pm 1}$ and the $2s$ levels when the exciton moves; the corresponding matrix element is linear in magnetic field. Then the repulsion of at least one level, say $2p_{-1}$, must lower its energy. In the weak-field limit this lowering is linear both in field and the momentum of the positron; hence, for small momenta it is larger in absolute value than the quadratic unperturbed kinetic energy of the positron. Thus, as the momentum increases the energy of this state should decrease, not increase. The energy minimum consequently is not at zero but at some finite projection of the momentum perpendicular to the magnetic field. In Fig. 6 we illustrate the energy of mixed $2p_{\pm 1} - 2s$ states of positronium as a function of the component of momentum transverse to the field, taking into account the diamagnetic energy obtained by solving the secular equation (the value of energy of the level for $H = 0$). The value of magnetic field (5×10^7 Oe) is here chosen so that when its is reexpressed in reduced units ($\hbar\omega_c/R_y$), it is close to the corresponding value of H used to plot similar functions in Fig. 4 for the case of excitons in Ge ($H = 2$ kOe). In Fig. 6, we show for comparison the same functions without including the magneto-Stark effect. A "pocket" is seen in the dispersion curve, i.e., a region of momentum where the energy is lower than that of positronium at rest. In Fig. 7 we
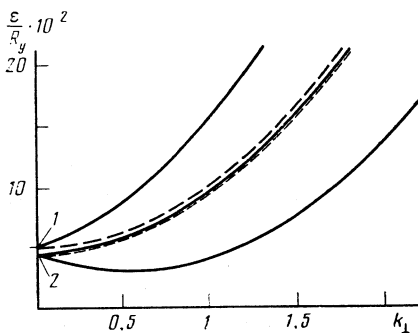
FIG. 7. Calculated functions $\rho(\varepsilon)$ for positronium with (continuous curve) and without (dashed curve) the magneto-Stark effect; $H = 50$ MOe.

illustrate the corresponding dependences of the density of states $\rho(\varepsilon)$.

The basic qualitative difference between positronium and excitons in Ge lies in the fact that for positronium, because of the equality of the electron and positron masses there is no linear Zeeman effect ($\gamma = 0$). The linear Zeeman effect in excitons gives a correction which is also proportional to the first power of the magnetic field, as in the case of the magneto-Stark effect; therefore, anomalous dispersion should be weak in excitons and entirely absent in hydrogen. In Fig. 4 we show the results of calculations of the dispersion of $2s$ and $2p_{\pm 1}$ states of excitons in Ge in a field $H = 2$ kOe. It is clear that the "pocket" for the $2p_{-1}$ state is extremely shallow: for small momenta the energy of the $2p_{-1}$ state is almost independent of momentum. We note that the value of temperature we chose for our experiments with excitons (1.6 K) corresponds to an equivalent temperature of ≈ 4000 K for positronium (these values are the same in reduced units of kT/R_y), and the value of $k_\perp$ shown in Fig. 6 for a positronium atom moving with the average thermal velocity is ≈ 1. Comparing the relative variations of energy of the $2p_{-1}$ levels under these conditions for excitons in Ge and positronium due to the magneto-Stark effect, we find that actually the effect of thermal motion on positronium is somewhat stronger.

An unexpected consequence of the shallow "pocket" in the dispersion law for the $2p_{-1}$ exciton band is an anomaly in the dependence of the latter's density of states on energy. In Fig. 8 we show the density of states $\rho(\varepsilon)$ with and without the magneto-Stark effect; it is noteworthy that in this case

FIG. 6. Calculated dependences of energy on $k_\perp$ for positronium states corresponding at $k = 0$ to the levels: 1—$2s$, 2—$2p_{\pm 1}$ (continuous curves). The same dependences without the magneto-Stark effect are represented by the dashed curves; $H = 0.5 \times 10^8$ Oe, k is given in units of $(2mkT)^{1/2}$ ($T = 4 \times 10^3$ K, $m = 2m_0$).
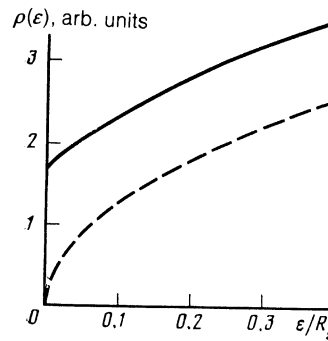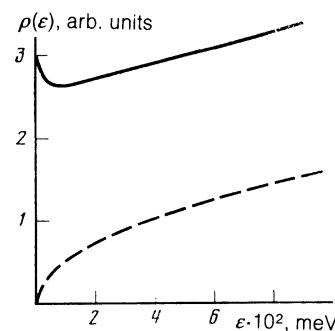
FIG. 8. Calculated functions $\rho(\varepsilon)$ for excitons with (continuous curve) and without (dashed curve) the magneto-Stark effect; $H = 2$ kOe.

the energy distribution function $f(\varepsilon) = \rho(\varepsilon)\exp(-\varepsilon/kT)$ differs markedly from $f(\varepsilon)$ in the absence of the magneto-Stark effect; one observes a maximum at $\varepsilon = 0$.

7. CONCLUSION

In this paper we have studied the Zeeman splitting of excitons in strained germanium in the range of small magnetic fields for the first time, and have shown that the magneto-Stark effect, which couples the center-of-mass motion to the internal motion of the exciton, significantly complicates the structure of the absorption spectrum. The strong influence of the magneto-Stark effect on the excited states of the exciton not only appreciably widens those lines of the spectrum which should be observable in the absence of the effect, but also leads to the appearance of new lines whose intensity and position in the magnetic field depend on temperature in a complicated way. It should be noted that these effects in Ge are observed even at low temperatures ($T \sim 1.6$ K) and small magnetic fields ($\hbar\omega_c/R_y$). This shows that the spectra of mobile multiparticle objects in semiconductors, e.g., excitons and excitonic molecules, are extremely complicated in a magnetic field, and that this complexity must be taken into consideration when their spectra are investigated with high-resolution laser spectroscopy using magnetic-field sweeping.

An important achievement of the theory proposed here is the prediction of anomalous dispersion caused by a magnetic field, and changes in the distribution function of excitons and positronium in the $2p_{-1}$ state, which should be observable in various experiments. We note that in positronium the magneto-Stark effect appears at magnetic fields that are significantly stronger ($H \gtrsim 10^7$ Oe) than those which are achievable under laboratory conditions.

$$\widetilde{H}_1 = (a^2 + 2|d|^2)^{1/2}\begin{pmatrix} 1 & 0 & 0 \\ 0 & 0 & 0 \\ 0 & 0 & -1 \end{pmatrix}$$

$$\widetilde{H}_2 = \frac{1}{a^2+2|d|^2} \times \begin{pmatrix} |d|^2 b_s + (a^2+|d|^2)b_p & a|d|(b_s - b_p) & |d|^2(b_s - b_p) \\ a|d|(b_s - b_p) & a^2 b_s + 2|d|^2 b_p & a|d|(b_s - b_p) \\ |d|^2(b_s - b_p) & a|d|(b_s - b_p) & |d|^2 b_s + b_p(a^2+|d|^2) \end{pmatrix}.$$

(A5)

Let Ω_I ($I = 1,2,3$) be eigenvalues of the matrix $H_1 + H_2$, and

$$\xi_I = (\xi_{I_1}, \xi_{I_2}, \xi_{I_3})$$

be real eigenvectors. Then for radiation with polarizations $e_{\pm} = \hat{x} \pm i\hat{y}$, the following relations hold:

$$\langle\psi_{1s}|e_+|\psi_I\rangle$$

$$= icd\left[\xi_{I_1}\frac{|d|}{\lambda_1(\lambda_1+a)} + \frac{\xi_{I_2}}{\lambda_1} - \xi_{I_3}\frac{|d|}{\lambda_1(\lambda_1-a)}\right] = icdF_{(+)},$$

$$\langle\psi_{1s}|e_-|\psi_I\rangle$$

$$= -icd^*\left[\xi_{I_1}\frac{|d|}{\lambda_1(\lambda_1-a)} - \frac{\xi_{I_2}}{\lambda_1} - \xi_{I_3}\frac{|d|}{\lambda_1(\lambda_1+a)}\right] = -icd^*F_{(-)}.$$

(A6)

APPENDIX: CALCULATING THE ABSORPTION LINE SHAPE

The Hamiltonian matrix in the $2p_{+1}$, $2s$, $2p_{-1}$ basis of states has the form

$$\hat{H} = \begin{pmatrix} b_p + a & d^* & 0 \\ d & b_s & d^* \\ 0 & d & b_p - a \end{pmatrix},$$

(A1)

where

$$b_s = \langle 2s|\mathcal{H}_D|2s\rangle, \qquad b_p = \langle 2p_{\pm 1}|\mathcal{H}_D|2p_{\pm 1}\rangle,$$
$$d = \langle 2s|\mathcal{H}_{\mu s}|2p_{\pm 1}\rangle, \qquad a = \langle 2p_{\pm 1}|\mathcal{H}_L|2p_{\pm 1}\rangle,$$
$$H_L = \frac{e\hbar}{2\mu_\perp c}\gamma H[\mathbf{rp}], \qquad \mathcal{H}_D = \frac{e^2}{8\mu_\perp c}[\mathbf{Hr}]^2$$

(A2)

we assume that for an exciton at rest $\varepsilon_{2s} = 2\varepsilon_{2p_{\pm 1}}$ (see section 5). So as to avoid complex values with H, it is convenient to go to a basis f_1, f_2, f_3 which diagonalizes the matrix H_1:

$$\hat{H} = H_1 + H_2 = \begin{pmatrix} a & d^* & 0 \\ d & 0 & d^* \\ 0 & d & -a \end{pmatrix} + \begin{pmatrix} b_p & 0 & 0 \\ 0 & b_s & 0 \\ 0 & 0 & b_p \end{pmatrix},$$

(A3)

which describes an exciton without including the diamagnetic energy. The eigenvalues and eigenvectors of the matrix H_1, are given by the equations

$$\lambda_1 = (a^2 + 2|d|^2)^{1/2}, \qquad f_1 = \frac{|d|}{\lambda_1}\begin{pmatrix} d^*(\lambda_1 - a)^{-1} \\ 1 \\ d(\lambda_1 + a)^{-1} \end{pmatrix},$$

$$\lambda_2 = 0, \qquad f_2 = \frac{a}{\lambda_1}\begin{pmatrix} -d^*/a \\ 1 \\ d/a \end{pmatrix},$$

(A4)

$$\lambda_3 = -\lambda_1, \qquad f_3 = \frac{|d|}{\lambda_1}\begin{pmatrix} -d^*(\lambda_1 + a)^{-1} \\ 1 \\ -d(\lambda_1 - a)^{-1} \end{pmatrix}.$$

In this basis,

In deriving these expressions we made use of the definition of the functions

$$\psi_{2p_{\pm 1}} = (\mp i)\frac{\exp(-r/2)}{2(16\pi)^{1/2}}(x \pm iy).$$

Here, c is a real matrix element; the quantities $f_{(\pm)}$ are also real and independent of the direction of the exciton momentum transverse to the field. The squared matrix element for linear polarization $e_x = \hat{x}$

$$|M|^2 = \frac{c^2}{4}\left[|d|^2(F_{(+)}^2 + F_{(-)}^2) - F_{(+)}F_{(-)}(|d|^2 + |d^*|^2)\right]$$

(A7)

contains two terms; the second is proportional to

$$|d|^2 + |d^*|^2 \sim k_x^2 - k_y^2, \tag{A8}$$

where **k** is the center-of-mass momentum of the exciton. The absorption line shape is given by the formula

$$I(\omega) \sim \sum_I \int d^2 k_\perp \exp(-k_\perp^2/2M_\perp kT) \, |M|^2 \delta[\omega - \Omega_I(\mathbf{k})]. \tag{A9}$$

It is clear that because of the isotropy of the total-mass tensor in directions perpendicular to the magnetic field, the second term in (A7) drops out. We can take damping into account by making the following replacement in (A9):

$$\delta(\omega - \Omega_I) \rightarrow \frac{1}{\pi} \frac{\Gamma}{(\omega - \Omega_I)^2 + \Gamma^2}. \tag{A10}$$

[1] E. M. Gershenzon, G. I. Gol'tsman, and N. G. Ptitsina, Pis'ma Zh. Eksp. Teor. Fiz. **16**, 228 (1972) [JETP Lett. **16**, 161 (1972)]; Pis'ma Zh. Eksp. Teor. Fiz. **18**, 160 (1973) [JETP Lett. **18**, 93 (1973)].

[2] E. M. Gershenzon, G. I. Gol'tsman, and N. G. Ptitsina, Zh. Eksp. Teor. Fiz. **70**, 224 (1976) [Sov. Phys. JETP **43**, 116 (1976)].

[3] V. S. Vavilov, N. V. Guseev, V. A. Zayats *et al.*, Pis'ma Zh. Eksp. Teor. Fiz. **17**, 480 (1973) [JETP Lett. **17**, 345 (1973)].

[4] N. V. Guseev, V. A. Zayats, V. L. Kononenko *et al.*, Fiz. Tekh. Poluprovodn, **8** [RUSSIAN WRONG], 1633 (1974) [Sov. Phys. Semicond. **8**, 1061 (1974)].

[5] T. Timusk, Phys. Rev. **B13**, 3511 (1976).

[6] N. O. Lipari and M. A. Altarelli Phys. Rev. **B15**, 4883 (1977).

[7] D. Labrie and T. Timusk, Phys. Rev. **B27**, 3605 (1983).

[8] M. Yamanaka, K. Muro, and S. Narita, J. Phys. Soc. Jpn. **44**, 1222 (1978).

[9] W. E. Lamb, Phys. Rev. **85**, 259 (1952).

[10] E. F. Gross, B. P. Zakharchenya, and V. V. Konstantinov, Fiz. Tverd. Tela 3, 305 (1961) [Sov.Phys. Solid State (Leningrad) **3**, 221 (1961)].

[11] I. I. Hopfield and D. G. Thomas, Phys. Rev. **122**, 35 (1961).

[12] K. Muro and Y. Nisida, Solid State Commun. **15**, 1663 (1974).

[13] V. D. Kulakovskii and V. M. Edel'shtain, Zh. Eksp. Teor. Fiz. **86**, 338 (1984) [Sov. Phys. JETP **59**, 195 (1984)].

[14] J. C. Hensel and K. Suzuki, Phys. Rev. **B9**, 4219 (1974).

[15] R. Faulkner, Phys. Rev. **184**, 713 (1969).

[16] V. D. Kulakovskii, I. V. Kukushkin, and V. B. Timofeev, Zh. Eksp. Teor. Fiz. **78**, 381 (1980) [Sov. Phys. JETP **51**, 191 (1980)].

[17] G. N. Gol'tsman, Pribory Tekh. Eksp. **1**, 136 (1972).

[18] T. G. Tratas and V. M. Edel'shtain, Zh. Eksp. Teor. Fiz. **81**, 696 (1981) [Sov. Phys. JETP **54**, 372 (1981)].

[19] W. Kohn and I. M. Luttinger, Phys. Rev. **98**, 915 (1955).

Translated by F. J. Crowne

1241   Sov. Phys. JETP 65 (6), June 1987

Gol'tsman *et al.*   1241